

INTERNATIONAL ATOMIC ENERGY AGENCY  
UNITED NATIONS EDUCATIONAL, SCIENTIFIC AND CULTURAL ORGANIZATION



INTERNATIONAL CENTRE FOR THEORETICAL PHYSICS  
34100 TRIESTE (ITALY) - P.O. B. 580 - MIRAMARE - STRADA COSTIERA 11 - TELEPHONE: 2240-1  
CABLE: CENTRATOM - TELEX: 406302-1

II4.SMR/204 - 17

WINTER COLLEGE ON  
ATOMIC AND MOLECULAR PHYSICS

(9 March - 3 April 1987)

Time-Resolved Fluorescence of Dyes of Bio-Medical Relevance:

Influence of the Environment

A. ANDREONI

Centro di Elettronica Quantistica e Strumentazione  
Elettronica del CNR  
Istituto di Fisica del Politecnico  
Milano, Italy

# PRIMARY PHOTO-PROCESSES IN BIOLOGY AND MEDICINE

at

The University of Padua Residence, Bressanone, Italy. 16th - 28th September 1984

TIME-RESOLVED FLUORESCENCE OF DYES OF BIO-MEDICAL RELEVANCE:

INFLUENCE OF THE ENVIRONMENT

Alessandra Andreoni

Department of Physics  
University of Milan  
Milano, 20133 Italy

## INTRODUCTION

In this lecture it is intended to provide a summary of the origins of the various fluorescence phenomena and to show, with some examples, what kind of information on biological systems thus becomes potentially available.

Efficient use of the various fluorescence phenomena to this practical end calls for appreciation of the competing processes involved in the formation and decay of the excited states, as well as of the influence of the intramolecular and intermolecular interactions upon them. Thus the possible fates of a Franck-Condon excited state of a fluorochrome will be briefly traced, with particular emphasis on the de-excitation pathways that are usually influenced by the biological environment. In fact, a rather general rule, which is followed by fluorochromes bound to biomolecules, is that some fluorescence properties of the dye are changed upon binding. When these changes are typical of a certain dye-biomolecule complex, the dye itself is called "fluorescent label" or "probe" of the biomolecule.

## ORIGINS OF THE FLUORESCENCE PHENOMENA

To discuss this point we will consider mainly the geometry of the excited state and the solvent shell. In general, following the absorption of one photon, the excess vibrational energy of  $S_1$ , i.e. the first excited singlet state of the fluorochrome, (Fig. 1 a) and b), is lost through exchange with the solvent molecules (thermal relaxation) at a typical rate of  $\sim 10^{12} \text{ s}^{-1}$ , or through partition among the degrees of freedom within the polyatomic excited molecule<sup>1</sup>. Normally, the decay from vibrational levels of higher excited electronic

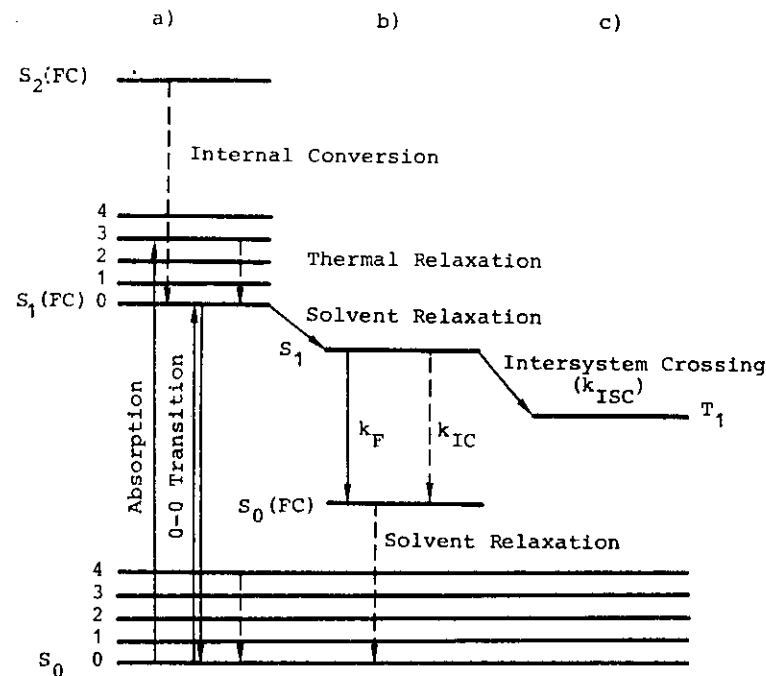


Fig. 1. Diagram of the energy levels and of the transitions for a dye molecule.

states ( $S_2$ ,  $S_3$ , etc.) proceeds via their own zero vibrational levels, which are attained through thermal relaxation, and internal conversion (radiationless transition) to the zero vibrational level of  $S_1$ . The internal conversion process is also very fast, with a rate of the order of  $10^{12} \text{ s}^{-1}$ <sup>2</sup>. The time-scale on which these non-radiative decay processes occur is too fast to be appreciably influenced by the environment of the fluorochrome.

Finally, the resultant zero level of  $S_1$  can decay by a variety of routes, which are also shown in Fig. 1 a). Let us first consider the fluorescence transition which, for an isolated molecule, has a rate, called radiative rate  $k_F$ , of  $10^7$  to  $10^9 \text{ s}^{-1}$ <sup>3,4</sup>. Since fluorescence occurs at room temperature from the vibrational levels of  $S_1$  that are close to the zero level, the most likely absorption transition is normally of greater energy; fluorescence in condensed media

displays a Stokes shift, or shift of the spectrum to longer wavelengths, in respect of the absorption. The 0-0 transition is seen to be of low probability, although it is the only one common to both absorption and fluorescence. Provided that the energy profiles of the  $S_1$ (FC) and  $S_0$  states in Fig. 1 a) are symmetrical in the region of interest, the 0-0 transition should act as a mirror of symmetry for the absorption and fluorescence spectra<sup>4</sup>. In practice, however, this may not occur, owing to significant alterations in molecular configuration in the excited state. Reorientation of solvent in response to these alterations or to dipole changes leads to a further lowering of the excited-state energy shown in Fig. 1 b), which results in a lack of spectral symmetry. In the ordinary solvents, reorientation occurs at rates of  $10^{11} - 10^{12} \text{ s}^{-1}$ <sup>5</sup>. The type as well as the amount, of the dye molecule alterations are closely related to the fluorochrome environment. Several mechanisms may be responsible for the configurational changes in dye molecules in the excited state  $S_1$ . Only the most relevant ones from the biological point of view will be discussed here: the excited-state complex formation and the excited-state proton transfer. Furthermore, competing with fluorescence are internal conversion processes ( $k_{IC} = 10^7 - 10^9 \text{ s}^{-1}$ , see Fig. 1 a) and b) ) that are not at all well understood, in which energy may again be dissipated to the solvent. Intersystem crossing (see Fig. 1 c) ) may occur towards lower-lying triplet levels ( $k_{ISC} = 10^8 \text{ s}^{-1}$ ) from  $S_1$  or, sometimes, from higher singlet states<sup>4</sup>. Both intersystem crossing and internal conversion are non-radiative processes that are influenced by the environment. The mechanisms through which these processes are made sensitive to the environment are of more general interest and discussed in many review papers<sup>3,5-7</sup>.

All processes so far considered are unimolecular. In practice, bimolecular processes also compete for the decay of  $S_1$ . They include resonance energy transfer, collisional and static quenching, concentration quenching, and self-absorption<sup>4,8</sup>. These will not be dealt with, though they are quenching mechanisms, but energy transfer in Acridines and static quenching in Porphyrins will be considered separately owing to the reach information they can provide.

#### FLUORESCENCE PARAMETERS OF INTEREST

For most chromophores, the environment acts only on the non-radiative decay pathways of the relaxed configuration of  $S_1$  (namely, intersystem crossing and internal conversion). Thus the overall non-radiative decay rate  $k_{NR}$  of the relaxed  $S_1$  configuration is modified by the binding, in general, while the radiative decay rate  $k_F$  is left unaltered<sup>4,6</sup>. This is typically the case where absorption measurements on the fluorescent label are not significant from the biological point of view, the absorption spectrum being related to  $k_F$ , which is rather insensitive to binding. The fluorescence properties of the label will, on the other hand, be influenced by the environment. In particular, even in the simplest case of first-order kinetics, both

the fluorescence decay time  $\tau$  and the fluorescence quantum yield  $\phi$

$$\tau = (k_F + k_{NR})^{-1} \quad (1)$$

and

$$\phi = k_F / (k_F + k_{NR}) \quad (2)$$

respectively, are parameters that may be sensitive to the environment, since they depend on  $k_{NR}$ . There are examples of dye-biomolecule complexes for which both  $\tau$  and  $\phi$  are either increased or decreased by the presence of a binding, as compared with the case of the free dye molecule. Of these, Acridines will be discussed here as a relevant example of this behaviour when they interact with DNA<sup>9</sup>.

Measurement of the fluorescence decay time  $\tau$ , at least as long as it falls within the nanosecond time-scale, is preferred to that of the fluorescence quantum yield  $\phi$ , due to the fact that an absolute evaluation of  $\phi$  is, in general, critical. The analysis of the time-resolved fluorescence, together with the measurement of absorption and fluorescence spectra, is also a good means of investigating the other processes mentioned in the previous section. Examples of solvent effects on Furocoumarins will be briefly mentioned, since they are dealt with in greater detail elsewhere in this book<sup>10</sup>.

#### EXAMPLES OF INFORMATION AVAILABLE FROM TIME-RESOLVED FLUORESCENCE SPECTROSCOPY

Time and space limitations obviously make it impossible to deal with all applications of time-resolved fluorescence techniques in biology and medicine. Only some of these will be illustrated by data

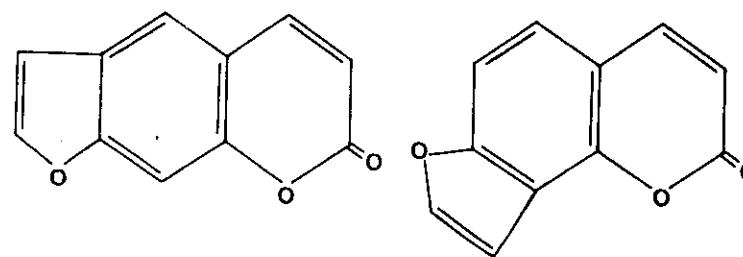


Fig. 2. Structures of linear (Psoralen) and angular (Angelicin) Furocoumarins.

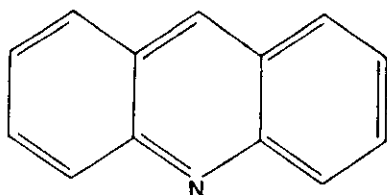


Fig. 3. Structure of the Acridine ring.

obtained in the author's laboratory\* on fluorescent probes that are also capable of reacting with the substrate, once they are brought to the excited state by the absorption of light. Kinetic studies of the singlet excited state are of increasing interest, particularly for molecules, such as Furocoumarins, whose photophysics is relatively little understood, though they are already used in photochemotherapy<sup>11</sup>. Recent results on both linear and angular Furocoumarins (see Fig. 2) have revealed the presence of complicating effects that cause these systems to depart from simple first-order kinetics. On the other hand, this is not surprising, since these molecules contain two chromophore moieties, i.e. the coumarin and the (benzo-)furan ring. We are now investigating to what extent the different exponential components that appear in the fluorescence decay are influenced by the solvent and by the binding to selected substrates<sup>10</sup>, with the aim of clarifying which excited-state configuration plays the most prominent role in the formation of DNA adducts<sup>11</sup>, which seems to be the mechanism responsible for their phototherapeutic activity.

Acridines are well-known specific stainings for nucleic acids<sup>12</sup>. Some of them bind only to double-helix DNA by intercalating the Acridine ring, which is sketched in Fig. 3, between two adjacent DNA base pairs, being held by van der Waals forces between the electron clouds of the bases and of the Acridine ring, with some ionic contribution of the charge localized on the heterocyclic nitrogen (see Fig. 3) and that of the phosphoric group in the DNA backbone<sup>9</sup>.

Most Acridines such as, for instance, Proflavine, Quinacrine, and Quinacrine Mustard, have fluorescence properties that depend on the base-pair composition of their binding site in the DNA; namely, when they intercalate two Adenine-Thymine (AT) pairs, their fluorescence quantum yield is higher, and the fluorescence decay time correspondingly longer (see eq.s (1) and (2)), than the values measured

\*Centro Elettronica Quantistica e Strumentazione Elettronica, C.N.R., Milano, Italy.

in buffer solution. On the contrary, the presence of a Guanine base in either of the two base pairs adjacent to the intercalated Acridine quenches its  $S_1$  state, with the consequent shortening of the fluorescence lifetime<sup>9</sup>. It must be noted that, while the increase in fluorescence is normally moderate for all Acridines, the decrease caused by the Guanine may be spectacular for some of them.

We measured the fluorescence decay of Quinacrine Mustard (QM) in Poly dA-Poly dT (i.e., a synthetic polynucleotide containing only AT-AT base-pair sequences) and in Poly dG-Poly dC (i.e., a polynucleotide made of Guanine-Cytosine base pairs, only) and compared it with the fluorescence decay of the same dye in phosphate buffer. With the excitation wavelength tuned at 419 nm, which corresponds to the absorption peak of QM in all these environments, and using the experimental apparatus previously described<sup>13</sup>, we measured 18 ns as the fluorescence decay time constant for QM in Poly dA-Poly dT, 3.9 ns for QM in the buffer solution used to stain the polynucleotides, and a faster decay of  $\sim 5$  ns time constant for QM in Poly dG-Poly dC. These data obtained by detecting the whole emission spectrum turned out to be in agreement with the values reported for the fluorescence quantum yield<sup>14</sup>, as calculated from eq.s (1) and (2). The same fast decay time constant appears in the fluorescence decay of Proflavine bound to Poly dG-Poly dC, which, on the other hand, is not as sensitive as QM to the binding to Poly dA-Poly dT. In fact, the same time constant of 4.3 ns was measured for Proflavine, both free in solution and bound to this polynucleotide<sup>15</sup>.

While it is generally accepted that the increase in the fluorescence lifetime for Acridines intercalating AT-AT sequences is due to the stiffening of the fluorochrome when it inserts itself between two adjacent DNA base pairs, which makes the internal conversion process less probable since it increases the  $k_{IC}$  rate (see Fig. 1 b), the reasons for the opposite behaviour of Acridines intercalated adjacently to a GC pair are still under discussion. The different explanations proposed can be reduced mainly to the two following possibilities: (i) charge-transfer complex formation, and (ii) excited-state proton transfer.

The fact that the chemical and physical characteristics of a fluorochrome are quite different in the electronically-excited state from those in the ground state is not surprising, since excitation by ultraviolet or visible photons involves perturbation of the electron cloud that determines the chemical bonding characteristics of all organic molecules. Actually, the spectrum-integrated fluorescence decay of QM in Poly dG-Poly dC could be fitted by two exponential components: besides the predominant one already mentioned, a second minor component could be found in this case, with a time constant of  $\sim 5$  ns<sup>9</sup>. Since this double-exponential decay was shown to originate from a single type of complex between QM and the polynucleotide, we suggested that this complex is an excimer<sup>4</sup> formed by the excited QM mole-

cule and the Guanine residue. Excimer fluorescence is actually known to decay following a double-exponential decay law<sup>4,7,8</sup>. In addition, this excimer could be predominantly of the charge-transfer type<sup>7</sup>, owing to the good electron-donor property of QM and electron-acceptor ability of Guanine<sup>16</sup>. The other possibility, that an excited-state proton transfer process might be responsible for the lifetime shortening of the Acridine excited state induced by the binding with Guanine, arises from observation of the time-resolved fluorescence spectrum of QM in buffer<sup>17</sup> and its comparison with that measured for the same dye bound to Poly dA-Poly dT or to Poly dG-Poly dC<sup>18</sup>. The fact that the protonation or deprotonation constants of a fluorochrome should depend on its particular excited state is also reasonable<sup>19</sup> and al-

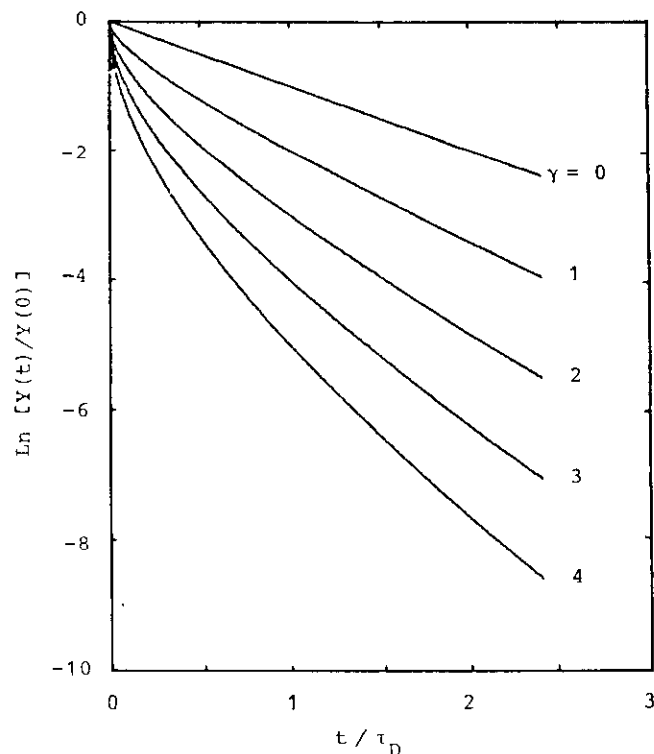


Fig. 4. Logarithmic plot of the calculated fluorescence decay of donors undergoing Förster energy transfer.  $\gamma$  is a parameter that is indicative of the process efficiency (see text).

ready demonstrated to occur for some Acridines<sup>12</sup>. Following this interpretation, each excited-state protonated species might be assigned a single fluorescence decay time constant and the fastest decaying species (.5 ns) could be formed preferentially by QM bound adjacently to Guanine, while the slowest decaying species (18 ns) is more likely to be formed by QM intercalating AT-AT sequences. Further time-resolved spectral measurements of the emission would certainly be helpful for substantiating this possible explanation.

Without going into greater detail as to the reasons for the DNA-base specificity of the Acridine fluorescence lifetime - and quantum yield, it is worthwhile summarizing here other aspects of the investigations on DNA chemical and structural properties, performed using these dyes as fluorescent probes. A natural DNA, that is the DNA of a given species whose base-pair sequences are fixed by nature, is an extremely interesting environment for Acridines, since it is a model in which the two classes of molecules, which differ in their excited-state lifetimes, coexist at relative distances of a few Angströms and are distributed as defined by the base-pair composition of the binding sites. Thus we may look upon Acridine-stained DNA as an ideal system for the study of the interactions between the two classes of fluorescent labels. For instance, the time-resolved fluorescence decay of QM staining a bacterial DNA should, in the absence of any interaction, be the superimposition of the 0.5 ns decay on the 18 ns decay. The relative amplitudes of the two components are expected to reflect the frequency in the DNA of AT-AT sequences in relation to that of sequences containing at least a Guanine: that is, both AT-GC and GC-GC together. The experimental fluorescence decay turned out to be different, - indeed, not even representable as the sum of exponential components, since it could more appropriately be fitted by the following law:

$$Y(t) = Y(0) \times \exp \left[ -(t/\tau_D) - \gamma(t/\tau_D)^{1/2} \right] \quad (3)$$

in which  $\gamma$  is a parameter that depends on the staining conditions (namely, on the DNA and QM concentrations<sup>20</sup>), but both  $\gamma$  and  $\tau_D$  are constant for all bacterial DNAs measured, regardless of their base-pair composition. Equation (3) is plotted for a few values of  $\gamma$  in Fig. 4.

The experimental results<sup>13</sup> show, therefore, that an interaction between the two populations of QM molecules does occur. Actually, eq. (3) suggests that the interaction is the Förster non-radiative energy transfer<sup>21</sup>, in which the QM molecules intercalating the AT-AT sequences act as donors of their excitation energy in favour of the molecules intercalated adjacently to a Guanine base, which have a much shorter excited-state lifetime. On the other hand, the subnanosecond pulses used in this experiment have the same probability of bringing to  $S_1$  the QM molecules of both populations, since the absorption spectrum of the fluorochrome is not modified by the base-pair composition of the binding site<sup>18</sup>. But, soon after the excitation pulse, the large

majority of QM molecules still excited are those intercalating AT-AT sequences; in this environment, these molecules can follow a new non-radiative decay pathway to release their excitation energy, being surrounded at very short distances in the natural DNA by other QM molecules in the ground state, to which they can transfer the excitation energy<sup>22</sup>. This obviously causes the donor fluorescence decay to depart from a single exponential decay (see Fig. 4), since the rate of this quenching mechanism depends on the donor-to-acceptor distances. In other words, the photons appearing at the beginning of the decay curves in Fig. 4 are emitted by the donors that have acceptor closer than those emitting later. This exchange of energy occurs through a dipole-dipole interaction whose rate is inversely proportional to the donor-to-acceptor distance. It can easily be shown that this fact makes the parameter  $\gamma$  appearing in eq. (3) extremely sensitive<sup>21</sup> to the average distance between QM molecules of the two classes. Furthermore, Fig. 4 shows that the shape of the fluorescence decay depends quite appreciably on the value of  $\gamma$ . This is the reason why analysis of the fluorescence decay curves of these probes provides such rich information on the chemical composition and structure of the stained DNA.

Porphyrins are a class of tetrapyrrolic dyes some of which, namely Hematoporphyrin (Hp) and a mixture known as Hematoporphyrin Derivative (HpD), were proposed many years ago as possible tumor photosensitizers<sup>23</sup>. The reasons for preferential localization in the tumor tissues (or cells) are fairly closely related to the hydrophobicity of these molecules that makes them to aggregate strongly in aqueous solutions. Hp is, notably, a molecule that exhibits hypochromicity when it aggregates (static fluorescence quenching). We studied the time-resolved fluorescence of Hp and HpD in aqueous solutions with increasing concentration and found that the fluorescence decay of Hp could be fitted by a single exponential of  $\sim 15$  ns time constant only at very low concentration values (below 2  $\mu$ M), but that, for increasing concentrations, a second faster decay component ( $\sim 3$  ns time constant) appeared with increasing initial amplitude<sup>24</sup>. As the aggregation equilibrium of Hp involves not only monomers and dimers, but also higher-order aggregates, we expected to detect further short-decay components with the increase in concentration, which did not happen, even at values as high as 100  $\mu$ M.

At this point it is worth noting that, from the fitting curve of a multiexponential decay, such as

$$Y(t) = \sum_i A_i \exp(-t/\tau_i) \quad (4)$$

the fluorescence quantum yield can easily be calculated as, from its definition<sup>4</sup>, is given by

$$\Phi = \left( \sum_i (\sigma_i N_i k_{Fi} \tau_i) \right) / \left( \sum_i (\sigma_i N_i) \right) \quad (5)$$

in which  $\sigma_i$  is the absorption cross-section at the excitation wave-

length of the  $i$ -th species, with radiative rate  $k_{Fi}$ , which is present in the concentration  $N_i$  and has a lifetime  $\tau_i$ . In our case, the different species are distinct because of the different degree of static quenching. If, as is often the case, the absorption spectra of the species have different profiles but similar integrals, their radiative rates  $k_{Fi}$  will be almost the same ( $k_F$ ) and eq. (5) can be rewritten as

$$\Phi = k_F \left( \sum_i A_i \tau_i \right) / \left( \sum_i A_i \right) \quad (6)$$

in which the values of  $A_i$  and  $\tau_i$  can be obtained from the fitting curve in eq. (4). Note that, in the case of a single-exponential decay, eq. (6) is reduced to eq. (2), taking into account eq. (1). According to eq. (6), we determined the values of  $\Phi$  in arbitrary units, since we did not compute  $k_F$  from the absorption data, for different Hp concentration values in the 2 - 100  $\mu$ M range, and compared these values with those obtained spectrophotometrically as the ratio of photons emitted to photon absorbed under cw excitation. The values obtained for  $\Phi$  from the decay-fitting curves decreased much slower<sup>24</sup> for increasing concentrations than did those obtained from the cw measurements. This has been interpreted as an indirect proof that the higher-order Hp aggregates fluoresce with lifetimes that are much shorter than the time resolution of our detection apparatus, which was  $\sim 200$  ps in this experiment. In fact, when computing the  $\Phi$  values according to eq. (6), it is possible to miss, in the nominator, the terms relating to the aggregates with undetectable decay times which, on the other hand, contribute to the absorption (i.e. to the denominator). For this reason, the use of eq. (6) can lead to an over-evaluation of the fluorescence quantum yield, particularly at high concentration values, where higher-order aggregates are present in large amounts.

HpD was investigated in a similar manner<sup>25</sup> with the main result that more stable aggregates, not only of hydrophobic origin, were present in this substance as compared with Hp, this being evidenced by measurements performed both in organic solvents of different polarity and in micellar systems.

A great deal of work has been done in the field of the time-resolved fluorescence spectroscopy of Porphyrins and related compounds, which has proved this technique to be a useful tool to distinguish between Porphyrins of different aggregational states<sup>26,27</sup>, binding sites<sup>28</sup> and, more recently, similar chemical structures<sup>29</sup>. As the physical reasons why these parameters influence the excited-state lifetime have not been clarified yet, these results are not discussed here, the aim of this paper having been to offer well-established examples of dye-biomolecule interactions that may influence the fluorescence lifetime of chromophores.

#### REFERENCES

1. K.F.Freed, Energy dependence of electronic relaxation processes

- in polyatomic molecules, in: "Radiationless Processes in Molecules and Condensed Phases," F.K.Fong, ed., Springer-Verlag, Berlin, Heidelberg, New York (1976).
2. P. Avouris, W.M. Gelbart and M.A. El-Sayed, Nonradiative Electronic Relaxation under Collision-Free Conditions, Chem. Rev. 77: 793 (1977).
  3. W.R. Ware, Kinetics of fluorescence decay: an overview, in: "Time-Resolved Fluorescence Spectroscopy in Biochemistry and Biology," R.B. Cundall and R.E. Dale, ed.s, Plenum Press, New York, London (1983).
  4. J.B. Birks, "Photophysics of Aromatic Molecules," Wiley-Interscience, New York, Sydney, Toronto (1970).
  5. R.A. Badley, Fluorescent probing of dynamic and molecular organization of biological membranes, in: "Modern Fluorescence Spectroscopy," Vol. 2, E.L. Wehry, ed., Plenum Press, New York, London (1976).
  6. T.C. Werner, Use of fluorescence to study structural changes and solvation phenomena in electronically excited molecules, in: "Modern Fluorescence Phenomena," Vol. 2, E.L. Wehry, ed., Plenum Press, New York, London (1976).
  7. J.B. Birks, Photophysics of aromatic molecules - a postscript, in: "Organic Molecular Photophysics," Vol. 2, J.B. Birks, ed., John Wiley & Sons, London, New York, Toronto, Sydney (1975).
  8. N. Mataga, Properties of molecular complexes in the electronic excited states, in: "Molecular Interactions," Vol. 2, H. Ratajczak and W.J. Orville-Thomas, ed., John Wiley & Sons, Chichester, New York, Brisbane, Toronto (1981).
  9. A. Andreoni, C.A. Sacchi and O. Svelto, Structural studies of biological molecules via laser-induced fluorescence: Acridine-DNA complexes, in: "Chemical and Biochemical Applications of Lasers," Vol. IV, C. Bradley Moore, ed., Academic Press, London, New York (1979).
  10. A. Andreoni, R. Cubeddu, F. Dall'Acqua, C.N. Knox and T.G. Truscott, Excited states of furocoumarins, in: "Primary Photoprocesses in Biology and Medicine," R.V. Bensasson, G. Jori, E.J. Land and T.G. Truscott, ed.s, Plenum Press, New York, London (1985).
  11. P.-S. Song and K.J. Tapley, Jr., Photochemistry and Photobiology of Psoralens, Photochem. Photobiol. 29:1177 (1979).
  12. A. Albert, "The Acridines," E. Arnold Ltd, London (1966).
  13. G. Bottioli, G. Prenna, A. Andreoni, C.A. Sacchi and O. Svelto, Fluorescence of Complexes of Quinacrine Mustard with DNA. I: Influence of the DNA Base Composition on the Decay Time in Bacteria, Photochem. Photobiol. 29:23 (1979).
  14. S.A. Latt and S. Brodie, Fluorescent probes of chromosome structure, in: "Excited States of Biological Molecules," J.B. Birks, ed., Wiley-Interscience, London, New York (1976).
  15. A. Andreoni, R. Cubeddu, S. De Silvestri, P. Laporta and O. Svelto, Time-Delayed Two-Step Selective Laser Photodamage of Dye-Biomolecule Complexes, Phys. Rev. Letters 45:431 (1980).
  16. E.D. Bergmann, The interaction of aromatic hydrocarbons with nucleic acids and their constituents, in: "Molecular Associations in Biology," B. Pullman, ed., Academic Press, New York, San Francisco, London (1968).
  17. A. Andreoni, R. Cubeddu, S. De Silvestri and P. Laporta, Time-Resolved Fluorescence Spectrum of Quinacrine Mustard, Opt. Commun. 33: 277 (1980).
  18. A. Andreoni, R. Cubeddu, S. De Silvestri and P. Laporta, Time-Resolved Fluorescence Spectrum of Quinacrine Mustard Bound to Synthetic Polynucleotides, Chem. Phys. Letters 80:323 (1981).
  19. L. Brand and W.R. Laws, Excited-state proton transfer, in: "Time-Resolved Fluorescence Spectroscopy in Biochemistry and Biology," R.B. Cundall and R.E. Dale, ed.s, Plenum Press, New York, London (1983).
  20. A. Andreoni, S. Cova, G. Bottioli and G. Prenna, Fluorescence of Complexes of Quinacrine Mustard with DNA. II: Dependence on the Staining Conditions, Photochem. Photobiol. 29:951 (1979).
  21. J.B. Birks, Energy Transfer in Organic Systems, VI. Fluorescence Response Functions and Scintillation Pulse Shapes, J. Phys. B (Proc. Phys. Soc.) 1:946 (1968).
  22. A. Andreoni, Lasers in microfluorometry and selective photobiology, in: "Lasers in Biology and Medicine," F. Hillenkamp, R. Pratesi and C.A. Sacchi, ed.s, Plenum Press, New York, London (1980).
  23. W. Hausmann, The Sensitizing Action of Hematoporphyrin, Biochem. Z. 30:176 (1911).
  24. A. Andreoni, R. Cubeddu, S. De Silvestri, G. Jori, P. Laporta and E. Reddi, Time-Resolved Fluorescence Studies of Hematoporphyrin in Different Solvent Systems, Z. Naturforsch. 38c:83 (1983).
  25. A. Andreoni, R. Cubeddu, S. De Silvestri, P. Laporta, G. Jori and E. Reddi, Hematoporphyrin Derivative: Experimental Evidence for Aggregated Species, Chem. Phys. Letters 88:33 (1982).
  26. A. Andreoni and R. Cubeddu, Properties of the Blue-Shifted Emission of Hematoporphyrin and Related Derivatives in Aqueous Solution, Chem. Phys. Letters 100:503 (1983).
  27. F. Ricchelli and L.I. Grossweiner, Properties of a New State of Hematoporphyrin in Dilute Aqueous Solution, Photochem. Photobiol. (in press).
  28. G. Bottioli, F. Docchio, I. Freitas, R. Ramponi and C.A. Sacchi, Hematoporphyrin derivative: fluorescence studies in solution and cells, in: "Porphyrins in Tumor Phototherapy," A. Andreoni and R. Cubeddu, ed.s, Plenum Press, New York, London (1984).
  29. A. Andreoni and R. Cubeddu, Photophysical Properties of Photofrin II in Different Solvents, Chem. Phys. Letters 108:141 (1984).

# A Semiconductor Detector for Measuring Ultraweak Fluorescence Decays with 70 ps FWHM Resolution

SERGIO COVA, SENIOR MEMBER, IEEE, ANTONIO LONGONI, ALESSANDRA ANDREONI, AND RINALDO CUBEDDU

**Abstract**—The performance of a new single-photon avalanche photodiode particularly suitable for the detection of fast and ultraweak light pulses is described. The advantages of this device over other available detectors are discussed. The electronic circuitry developed allows the measurement of fluorescence decays with a time resolution of 70 ps FWHM (full-width at half-maximum) and a data acquisition rate of up to 50 kHz.

## I. INTRODUCTION

THE development of laser techniques for generating ultra-short light pulses at wavelengths from UV to IR has stimulated studies of ultrashort fluorescence phenomena in various fields, particularly in photochemistry and molecular biology. The difficulty of obtaining very short time resolution in measurements of fluorescence decay times is often increased by the low intensity of the light to be detected. The intensity

level has to be evaluated with reference to the number  $N_{DR}$  of detected photons per resolving time  $T_R$  of the measurement. In order to obtain measurements having a high signal-to-noise ratio ( $S/N$ ) with moderate or low  $N_{DR}$ , say with  $N_{DR} < 10^4$ , the measurement apparatus, besides having a short  $T_R$ , must: 1) have *averaging* capability, that is, it must accumulate the data obtained from many repetitions of the fluorescence pulse so that fluctuations due to the radiation statistics can be averaged out; 2) employ *photodetectors with high internal amplification*  $A_D$ , that is, transduction systems where one detected photon is transduced into a high number  $A_D$  of electrical conduction carriers (free electrons or electron-hole pairs). This requirement arises because of the electrical noise in the circuits of the measurement apparatus. In fact, in order to avoid degradation of the information carried, the electrical signal should be much higher than this noise, so that the lower the  $N_{DR}$ , the higher the required  $A_D$ .

The shortest resolving times among electronic methods, a few picoseconds, are provided by streak cameras. Some pre-amplification is provided in such apparatus by the accelerating voltage, and further amplification may be provided by the

detector system (image intensifiers, etc.) used to "read" the output screen. This fact and the averaging capability, provided by the progress in scan synchronization, have made possible the extension of their measurement range down to moderately low intensities. However, they still have various drawbacks; the resolving time is proportional to the time range scanned, so that the highest resolution is obtained only on very short ranges (about 1 ns), the linearity is not very high, and the apparatus is fairly costly and cumbersome.

In fact, electronic methods employing photodetectors are often preferred to streak cameras in all cases where their resolution is sufficient for the measurement envisaged. Ultrafast photodiodes, with resolutions of the order of 50 ps full-width at half-maximum (FWHM), are commercially available, but the lack of internal amplification (one detected photon produces one electron-hole pair) makes them unsuitable for fluorescence measurements and limits their application to monitoring of laser pulses. Ultrafast avalanche photodiodes (APD) have internal amplification in the range  $A_D = 10$ –100, and may therefore also be used at moderate intensity levels, say  $N_{DR} > 10^3$ , with resolving times down to about 100 ps. However, in most cases the fluorescence intensity to be detected is weak ( $N_{DR} < 100$ ) or ultraweak ( $N_{DR} < 10$ ), down to the single-photon level, and detectors with an internal gain  $A_D$  higher than  $10^4$  are required.

Such high gains are obtained in various types of photomultiplier tubes (PMT's) by means of cascaded secondary electron emission. The results obtained can be readily analyzed by making reference to the elementary current pulse, corresponding to the detection of a single photon (SP), called single (photo-) electron response SER [1], [2]. The most relevant SER parameters are: 1) the width  $\sigma_w$  of its waveform, 2) the delay  $t_c$  of its centroid with respect to the arrival time of the photon, and 3) the jitter  $\sigma_c$  of this delay. The measurement of a fluorescence decay can be performed either by measuring the waveform of the detector current pulse (waveform sampling and averaging techniques), or by measuring the time position of the SER pulses with respect to the pulsed excitation of the fluorescence and accumulating a histogram of many such measurements (single-photon timing or time-correlated single-photon counting [2], [3]). The detector contribution [2] to the resolving time is  $\sqrt{\sigma_w^2 + \sigma_c^2}$  in waveform averaging, while it is just  $\sigma_c$  in SP timing. Since  $\sigma_w$  is considerably greater (5–10 times) than  $\sigma_c$  for all PMT types, the time resolution of SP timing is definitely higher. In order to employ this technique, however, it is necessary to work with a very low detected intensity [2], [3], much less than one detected photon per excitation pulse on the average, and, therefore, it is often necessary to deliberately attenuate the available light. This is a waste of information, which must be recovered by accumulating measurements over a large number of excitation pulses. If the repetition rate of such pulses is low, say less than 1 kHz, as it is in the case of nitrogen lasers, the real time taken by the experiment may be impractically long. On the other hand, if the available repetition rate is high, as in the case of CW mode-locked and cavity-dumped dye lasers, there is no practical problem in collecting a large number of measurements.

The resolution actually obtained depends on the PMT type.

Discrete-dynode electrostatically focused PMT's have high gains  $A_D$ , up to  $10^6$ . Resolutions from 350 to 500 ps FWHM have been observed by various experimenters [4], [5], and values down to 230 ps have been reported [6] for selected PMT samples. A drawback observed in most of the electrostatically focused PMT types is the presence of small secondary peaks [7] in the resolution curve (which can be accurately obtained by measuring the waveform of ultrashort light pulses) that complicate the analysis of fluorescence curves. Crossed electric and magnetic field focused PMT's have low gain, on the order of  $10^3$ , so that although in principle they can be expected to provide resolutions on the order of 50 ps, in practice 230 ps have been observed [8] at best, due to the noise contribution in the electronic amplifying and timing circuits. PMT types based on microchannel-plate (MCP) multipliers have gains ranging from  $10^3$  to  $10^7$  and can be expected to provide less than 100 ps FWHM resolution. Measured resolutions have been reported for various PMT-MCP models [9], [10], most of them from 130 to 200 ps. A value of 70 ps has also been reported [11], but with a resolution curve affected by a slow low-level tail. In any case, the application of MCP-PMT's is still hampered by various problems, a major one being the degradation of the photocathode quantum efficiency that results in a limited working life of the device.

Single-photon detection can also be obtained with specially devised types of semiconductor photodiodes [12]–[16] called single-photon avalanche diodes (SPAD's). They can be biased above the breakdown voltage, and a nonproportional self-sustaining avalanche current can be triggered by the absorption of a single photon. The timing jitter in the avalanche triggering may be expected to be on the order of the transit time of carriers in the junction, which can be as low as a few tens of picoseconds. However, for several years the practical application of such devices has been severely restricted by drawbacks due to the simple passive method traditionally used to terminate the avalanche current triggered by the photon [12]–[16]. This fact, together with specific features of the devices and the electronic equipment used, contributed to degrade to about 1 ns the resolution actually observed by other experimenters [17]. The active-quenching method, devised by Cova and Longoni (see, e.g., [15] or [16]), has removed these drawbacks and opened the way to wider application and better understanding of these devices. In this paper, the prospective application of these devices to the measurement of fluorescence decay times shorter than 100 ps is dealt with, on the basis of results obtained in experiments performed with a CW synchronously pumped mode-locked rhodamine 6G dye laser.

## II. STRUCTURE AND OPERATION OF SINGLE-PHOTON AVALANCHE DIODES

The geometry and physical structure of suitable diodes must be such that local concentrations of high electrical fields are avoided, so that the breakdown is uniform over the junction area. The diodes used in the present work have the geometry described by Haitz [12] and outlined in Fig. 1. The avalanche region, where the carriers find the electric field sufficient to trigger a breakdown, is the  $n^+p$ -junction formed by a shallow ( $\sim 0.3 \mu\text{m}$ )  $n^+$  layer. Illumination is from the top in Fig. 1.

Manuscript received August 4, 1982.

S. Cova and A. Longoni are with the Istituto di Fisica del Politecnico, Milano, Italy.

A. Andreoni and R. Cubeddu are with the Centro di Elettronica Quantistica e Strumentazione Elettronica del CNR, Milano, Italy.



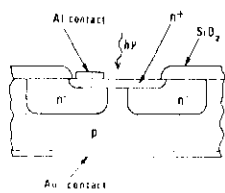


Fig. 1. Schematic cross section of the SPAD's tested.

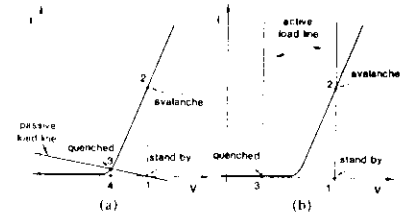


Fig. 2. (a) Passive quenching, provided by a high load resistor. 1-2: Avalanche triggering by a carrier. 2-3: Voltage drop due to discharge of the diode capacitance by the avalanche current. 3-4: Avalanche quenching. 4-1: Slow voltage recovery due to recharge of capacitance through the load resistor. (b) Active quenching, with a low-impedance bias source controlled in an active feedback arrangement. 1-2: Avalanche triggering by a carrier. 2-3: Fast quenching transition, forced by the load-line shift provided by the circuit. 3-1: Fast recovery, forced by the circuit.

The breakdown region is surrounded by a deep-diffused (5-8  $\mu\text{m}$ )  $n^+$  guard ring. The diameter of the p-type plug thus defined is kept small; therefore, most of the electrons generated in the neutral p-region (by photon absorption and thermal generation) are drained by the wide low-field  $n^+$ -p-junction, whose breakdown voltage is higher than that of the  $n^+$ -p-junction. The probability of triggering an avalanche is high only for electrons generated in the  $n^+$ -p depletion layer and within a few microns from it in the neutral p-region. The samples tested [16] were made with conventional planar technology on p-type Si wafers with  $0.7 \Omega \cdot \text{cm}$ , so that the breakdown voltage of the  $n^+$ -p-region was around 30 V. The diameters of the active areas ranged from 10 to 65  $\mu\text{m}$ .

The current-voltage curve of the diodes is sketched in Fig. 2. When biased above the breakdown voltage, the device can be either in a quiescent state with negligible current, or in a high current state with a self-sustaining avalanche breakdown. The slope of the avalanche branch of the curve corresponds to resistance values on the order of a few kilohms, so that avalanche currents on the order of 1 mA are obtained from devices biased a few volts above the breakdown voltage. The transition from the quiescent to the avalanche state can be triggered by a single free carrier in the depletion layer. If quenching is then provided by some arrangement, the device is reset to the zero current level and the current pulse is terminated. Such quenching was traditionally obtained [12]-[14] simply by using a high load resistor (100 k $\Omega$  or more) connected between the diode and the bias voltage source. This *passive* quenching method is outlined in Fig. 2(a). The voltage drop 2-3 takes around 100 ns, and the voltage recovery 4-1 is longer by several microseconds because of the low recharging current

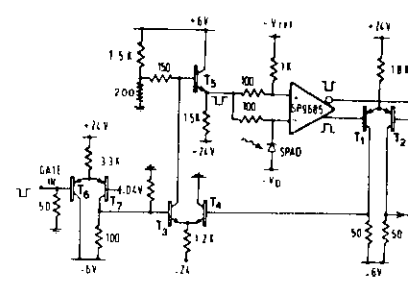


Fig. 3. Simplified diagram of the active-quenching circuit used in this work.

through the high resistor. Drawbacks arise because of the long duration of the cycle and because the avalanche can also be triggered by photons arriving during the recovery from previous pulses [15], [16]. In fact, during the recovery the device operates in perturbed conditions, with lower detection efficiency, lower multiplication, and correspondingly lower amplitude and higher fluctuations, so that the timing jitter is remarkably increased. If the repetition rate of background pulses due to stray light and thermal generation of carriers in the device is not low, photons to be timed have a nonnegligible probability of arriving during recovery from previous pulses, and the time resolution in the measurement is correspondingly degraded.

The *active-quenching* method [15], [16], devised in order to eliminate the drawbacks mentioned and operate the device with short well-controlled dead times, is outlined in Fig. 2(b). The quenching transition 2-3 is forced a few nanoseconds after the triggering 1-2 and takes about 2 ns. The device can be held in the off state 3 for a controlled time that can be as short as a few nanoseconds; the reset transient 3-1 then takes about 2 ns. The controlled low-impedance biasing arrangement also makes it easy to gate the device on or off by means of a fast external command [18].

The active-quenching circuit used in the present tests is shown in Fig. 3. With respect to previous circuits [15], [16], it has some practical advantages and better performance [18]. In fact, it does not require trimming when the SPAD sample is changed and is also suitable for SPAD samples with high breakdown voltages. Furthermore, the fast rise time of the avalanche current is better exploited in order to obtain the best possible timing jitter. As shown in Fig. 3, a fast gate control is also implemented.

### III. EXPERIMENTAL TESTS AND RESULTS

Experiments were performed by using a mode-locked rhodamine 6G dye laser synchronously pumped by an argon-ion laser. The time duration of the dye laser pulses was measured by SHG autocorrelation function, and was found to be less than 5 ps FWHM, assuming a Gaussian shape. Resolution tests were performed by directly measuring the laser pulse shape. The suitability of SPAD's to the measurement of fluorescence was then tested by measuring fast fluorescent decays excited by the laser pulses. A conventional electronic setup for time-correlated single-photon counting was used in the measurements [2]-[4]. A homemade [19] time-to-pulse-height con-

verter (TPHC) and a Silena BS27 multichannel pulse-height analyzer (MCA) were used to measure the delay distribution of the detected single photons with respect to the reference start pulses synchronized with the laser pulses. The start pulses were obtained by using a beam splitter and an ordinary fast photodiode with fast electronic circuitry. Measurements were performed both with and without a pulse picker on the laser beam. In experiments without the pulse picker, the repetition rate of the start pulses at the TPHC input was reduced to levels from 5 to 50 kHz by suitable demultiplying circuits. The use of the pulse picker allowed such repetition rates to be obtained directly for the light pulses. The synchronism jitter was initially checked by using a photodiode-circuit setup, identical to that in the start channel, in the stop channel. The observed FWHM was about 20 ps with the pulse picker and between 35 and 70 ps without it depending on various side effects.

The resolution curve obtained with laser pulses at 571 nm wavelength is shown in Fig. 4. The FWHM is 70 ps; this performance resulted from studies on the behavior of the device [20] and from the use of the new circuit, which made it possible to operate the device at higher voltages.

The resolution curve also has a slow low-level tail that can be better evaluated in a logarithmic plot, as shown in Fig. 5(a). This tail is due to diffusion [16] of the carriers generated in the neutral p-region beneath the depletion layer (see Fig. 1 and Section I). The intensity and steepness of the tail depend on the wavelength  $\lambda$  of the detected radiation because of the dependence on  $\lambda$  of the optical absorption length in silicon. This fact is certainly a drawback and may complicate the analysis of fluorescence measurements. However, in the present SPAD structure, the tail effect is not very significant in the wavelength range below 500 nm, as shown by the experimental example in Fig. 5(b). Furthermore, the carrier-diffusion effect is also found in ordinary photodiodes and avalanche photodiodes, and it is known that it can be strongly reduced by using suitably modified device structures (e.g., see [21]).

Solutions of various dyes, i.e., DODCI, erythrosin B, rhoda-

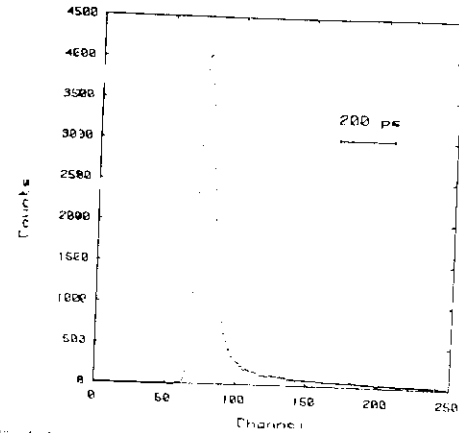


Fig. 4. Linear plot of the resolution curve, measured with 5 ps laser pulses at 571 nm wavelength. Time scale is 5.16 ps/channel.

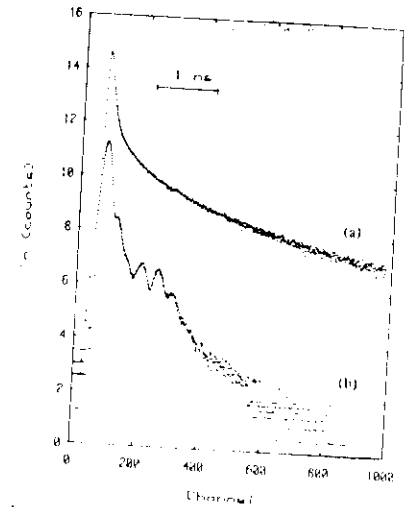


Fig. 5. Logarithmic plot of the curves measured with: (a) 5 ps laser pulses at 571 nm wavelength (same as Fig. 4); (b) 103 ps pulses at 476.5 nm wavelength of a mode-locked argon-ion laser. The small peaks on the tail are not due to the SPAD, but to small delayed spurious laser pulses that depend on the laser alignment.

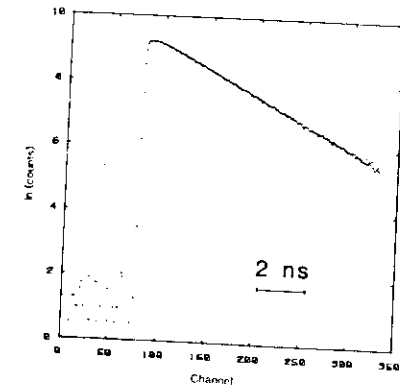


Fig. 6. Fluorescence decay of  $10^{-5}$  M rhodamine B (rhodamine 610 Perchlorate-Exciton, Inc.) in ethanol. Time scale is 46.94 ps/channel. Measured decay time constant is 2.99 ns.

mine B, and rhodamine 6G, either in ethanol or in water, were used as tests for fluorescence decay measurements. The samples were placed in a quartz cuvette and the fluorescence was measured at  $90^\circ$  through cutoff filters by the detector placed about 1.5 cm away from the excitation beam. No optical device was used to improve the light collection efficiency on the sensitive area (about 35  $\mu\text{m}$  diameter). The incident light intensity was adjusted so that the average number of detected photons per pulse was less than 0.1, as required for measurements of single-photon delay distribution [2], [3]. A representative experimental result obtained with rhodamine B  $10^{-5}$  M in ethanol is shown in Fig. 6. The fluorescence

decay time was found to be 2.99 ns, in agreement with the values reported in the literature [4].

#### IV. CONCLUSIONS

The results obtained demonstrate that SPAD's can be effectively used for measurements of very low-intensity fluorescence decays with the time-correlated single-photon counting technique, and that for such measurements they provide the highest time resolution available today. Besides high time resolution, SPAD's have other attractive properties: their resolution curve is free from the small secondary peaks observed with many PMT's; the wavelength range covered by their spectral sensitivity is more extended than that of PMT's, in particular, on the long wavelength side; the device is small and rugged and operates with low supply voltage and power dissipation; and gated operation under the control of fast low-voltage pulses is possible and practical.

The principal drawback of SPAD's is the presence of wavelength-dependent tails in the resolution curve, which limit the performance of this device in the measurement of decay curves containing more than one exponential component, in particular for emissions at wavelengths longer than 500 nm. However, developments in the device design and technology may be expected to improve the detector performance in this respect. In fact, by using more complicated device structures [21], it is possible to avoid to a great extent the collection, at the active (avalanching) junction, of carriers generated outside the depletion layer, but of course, at the expense of a reduction of the detection efficiency at long wavelengths.

In comparison with PMT's, the smaller sensitive area is a limitation. In many instances, however, it is possible to focus the emitted light on such an area; in other cases, the drawback is reduced by the ease of placing a small rugged detector close to the emission source. Furthermore, an increase in the diameter of the sensitive area to about 1 mm could be within the reach of expected technological developments.

Other studies and experiments in progress suggest that the resolution obtained in practice from SPAD's may be further improved toward the expected theoretical values, possibly with new device structures. Developments in the fast circuits associated with SPAD's may also be helpful. In conclusion, although SPAD's cannot be expected to replace PMT's in all applications, they deserve the attention of experimenters interested in ultrashort light pulses, and justify further development efforts.

#### ACKNOWLEDGMENT

The authors wish to thank G. Soncini and S. Solmi of the LAMF-CNR Laboratory for supplying device samples, G. Ghelmi for the skillful work in electronic circuit building and testing, and S. De Silvestri and P. Laporta for assistance in the operation of the laser system and fluorescence measurements.

#### REFERENCES

- [1] S. Donati, I. Gatti, and V. Svetko, "The statistical behavior of the scintillation detector: Theories and experiments," in *Advances in Electronics and Electron Physics*, vol. 26, L. Marton, Ed., New York: Academic, 1969.
- [2] S. Cova, M. Bertolaccini, and C. Bassolati, "The measurements of luminescence waveforms by single-photon techniques," *Phys. Status Solidi A*, vol. 18, pp. 11-62, July 1973.
- [3] M. R. Ware, *Creation and Detection of the Excited State*, A. Lamola, Ed., New York: Marcel Dekker, 1971.
- [4] V. J. Koester and R. M. Dowben, "Subnanosecond single-photon counting fluorescence spectroscopy using synchronously pumped tunable dye laser excitation," *Rev. Sci. Instr.*, vol. 49, pp. 1186-1191, Aug. 1978.
- [5] B. Leskovar and C. C. Lo, "Time resolution performance studies of contemporary high speed photomultipliers," *IEEE Trans. Nucl. Sci.*, vol. NS-25, pp. 582-590, Feb. 1978.
- [6] D. Bebelaar, J. J. F. Ramackers, M. W. Leeuw, R. P. H. Bettschnick, and J. Langelaar, "Application of a picosecond dye laser to the study of single rotational levels in 5-tetrazine vapour," in *Proc. 2nd Int. Symp. on Ultrafast Phenomena in Spectroscopy*, Reinhardtbrunn, East Germany, 1980, vol. 2, Akad. der Wiss. der DDR, Jena, 1981, pp. 213-217.
- [7] S. G. Stevens and J. W. Longworth, "Late output pulses from fast photomultipliers," *IEEE Trans. Nucl. Sci.*, vol. NS-19, pp. 356-359, Feb. 1972.
- [8] V. J. Koester, "Improved timing resolution in time-correlated photon counting spectrometry with a static cross-field photomultiplier," *Anal. Chem.*, vol. 51, pp. 458-459, 1979.
- [9] C. C. Lo and B. Leskovar, "Studies of prototype high-gain microchannel plate photomultipliers," *IEEE Trans. Nucl. Sci.*, vol. NS-26, pp. 388-394, Feb. 1979, and "Performance studies of high gain photomultipliers having Z-configuration of microchannel plates," *IEEE Trans. Nucl. Sci.*, vol. NS-28, pp. 698-704, Feb. 1981.
- [10] T. Hayashi, "Recent developments in photomultipliers for nuclear radiation detectors," *Nucl. Instrum. Methods*, vol. 196, pp. 181-186, May 1982.
- [11] I. Yamazaki, T. Murao, and K. Yoshihara, "Subnanosecond fluorescence lifetimes of pyrazine- $h_8$  and - $d_8$  vapor for photo-selected vibrational levels in the  $S_1(n, \pi^*)$  state," *Chem. Phys. Lett.*, vol. 87, pp. 384-388, Apr. 1982.
- [12] R. H. Hartz, "Model for the electrical behavior of a microplasma," *J. Appl. Phys.*, vol. 35, pp. 1370-1376, May 1964, and "Mechanisms contributing to the noise pulse rate of avalanche diodes," *J. Appl. Phys.*, vol. 35, pp. 3123-3131, Oct. 1965.
- [13] R. J. McIntyre, "The distribution of gains in uniformly multiplying avalanche photodiodes: Theory," *IEEE Trans. Electron Devices*, vol. ED-19, pp. 703-712, Jun. 1972.
- [14] W. O. Oldham, R. R. Samuelson, and P. Antognetti, "Triggering phenomena in avalanche diodes," *IEEE Trans. Electron Devices*, vol. ED-19, pp. 1056-1060, Sept. 1972.
- [15] P. Antognetti, S. Cova, and A. Longoni, "A study of the operation and performance of an avalanche diode as a single-photon detector," in *Proc. 2nd Ispra Nucl. Electron. Symp.*, Euratom Publ. EUR 5370e, 1975, pp. 453-456.
- [16] S. Cova, A. Longoni, and A. Andreoni, "Towards picosecond resolution with single-photon avalanche diodes," *Rev. Sci. Instr.*, vol. 52, pp. 408-412, Mar. 1981.
- [17] W. Eichner and W. Haecker, "Time resolution of Ge avalanche photodiodes operating as photon counters in delayed coincidence," *Rev. Sci. Instr.*, vol. 47, pp. 374-377, Mar. 1976.
- [18] S. Cova, A. Longoni, and G. Ripamonti, "Active-quenching and gating circuits for single-photon avalanche diodes (SPAD's)," *IEEE Trans. Nucl. Sci.*, vol. NS-29, pp. 599-601, Feb. 1982.
- [19] M. Bertolaccini and S. Cova, "The logic design of high precision time-to-pulse height converters, Part 2: A converter design based on the use of integrated circuits," *Nucl. Instrum. Methods*, vol. 121, pp. 557-566, Nov. 1974.
- [20] S. Cova, A. Longoni, and G. Ripamonti, to be published.
- [21] J. Muller, "Photodiodes for optical communications," in *Advances in Electronics and Electron Physics*, vol. 55, L. Marton, Ed., New York: Academic, 1981.

Sergio Cova (M'71-SM'82), photograph and biography not available at the time of publication.

Antonio Longoni, photograph and biography not available at the time of publication.

Alessandra Andreoni, photograph and biography not available at the time of publication.

Rinaldo Cubeddu, photograph and biography not available at the time of publication.